**Endocrine,** *vol. 27, no. 1, 1–9, June 2005* 0969–711X/05/27:1–9/$30.00 

# In Vivo Biological Activity of Exendin (1–30)

Máire E. Doyle,[1] Patrick McConville,[2] Michael J. Theodorakis,[1]
Margaret M. Goetschkes,[3] Michel Bernier,[1] Richard G. S. Spencer,[2]
Harold W. Holloway,[4] Nigel H. Greig,[4] and Josephine M. Egan[1]

*Diabetes Section National Institute on Aging, National Institutes of Health. [1]Diabetes Section, [2]NMR Unit, and [4]Drug Design and Development Section, National Institute on Aging, National Institutes of Health, 5600 Nathan Shock Drive, Baltimore MD 21224; and [3]Pathology Services Inc., 640 Memorial Drive, Cambridge, MA 02139*

**Activation of the glucagon-like peptide-1 (GLP-1) receptor on pancreatic beta cells by GLP-1 and exendin-4 (a more potent and stable agonist of the GLP-1 receptor than GLP-1) increases insulin secretion. Exendin-4 is 39 amino acids long, unlike GLP-1 which has 30 amino acids. Because of its non-mammalian (lizard) origin and unique C-terminal sequence, exendin-4 may be immunogenic in humans. We showed previously that the C terminally truncated exendin peptide exendin (1–30) has a reduced affinity for the GLP-1 receptor and a diminished ability to increase intracellular cAMP in insulinoma cells. Here we show that daily intraperitoneal injection of exendin (1–30) (1 nmol/kg) for 20 d followed by 31 d twice daily to *Lepr$^{db}$/Lepr$^{db}$* (*db/db*) mice significantly reduced the amount of visceral fat relative to saline-treated controls and improved $HbA_{1C}$ (control 9.5 ± 0.2% vs treated 7.9 ± 0.2%, $p = 0.001$) but was not as effective as exendin-4. To examine the ability of exendin (1–30) to stimulate beta-cell growth, we injected one group of 3-mo-old Fisher rats with exendin (1–30) (1 nmol/kg) and another group with saline for 8 d. We observed no change in beta-cell area, but did see a change in the number of islets with nuclei positive for BrdU [10.7 ± 1.8% exendin (1–30) vs 6.5 ± 0.5% control].**

**Key Words:** Rodents; magnetic resonance imaging; diabetes; insulinotropic compounds.

## Introduction

GLP-1 is an incretin hormone secreted from specialized enteroendocrine cells, primarily of the distal small intestine, in response to nutrient ingestion and is a key regulator of postprandial blood glucose levels *(1,2)*. It inhibits gastric emptying *(3)*, glucagon secretion *(4)*, and endogenous glucose production *(5)*, and augments glucose induced insulin synthesis and secretion *(6)*. It has also been shown to initiate beta (β)-cell proliferation followed by differentiation, through promotion of the transcription and synthesis of the β-cell transcription factor pancreatic duodenal homeobox-1 protein (PDX-1) in rodent models of diabetes *(7,8)*. Although expansion of β-cell mass has not been demonstrated in humans, there is indirect evidence of improved β-cell function in the type 2 diabetic state following GLP-1 treatment. Continuous infusion of GLP-1 can restore first-phase insulin secretion and induce "glucose competence" in β-cells, so that blood glucose is lowered *(9)* in the type 2 diabetic state. Thus, agonists of the GLP-1 receptor are now being developed by several pharmaceutical companies *(10)*. Dipeptidyl peptidase IV (DPP IV) rapidly cleaves the first two N-terminal amino acids of GLP-1, making it inactive as an insulinotropic peptide, a process that occurs at the site of production of GLP-1, the gut *(11)*. When GLP-1 is given continuously, an elevated steady state of intact GLP-1 is reached, and so increased insulinotropic activity is maintained long term *(9)*. However, continuous GLP-1 infusion is not very practical for everyday control of hyperglycemia.

Exendin-4 is a GLP-1 receptor agonist that is a more potent and longer lasting insulinotropic peptide than GLP-1 *(12–14)*. The 10-fold increase in the potency of exendin-4 in vivo relative to GLP-1 *(15)* is due to two factors: (a) an increased metabolic stability as the compound is resistant to cleavage by DPP IV and many of the neutral endopeptidases that degrade GLP-1 *(16)* and (b) secondly to its increased affinity for the GLP-1 receptor *(12,17,18)*. Exendin-4 is being assessed in clinical trials as a potential treatment for hyperglycemia *(10,15,19–21)*. Exendin-4 and GLP-1 share a 53% amino acid sequence homology with the major difference between them being in the nine amino acid C terminal sequence of exendin-4 (PSSGAPPPS), not present in GLP-1 (Table 1). Recent studies of the solution NMR structure of the peptides show that, although both GLP-1 and exendin-4 exhibit a highly helical tertiary structure, that of exendin-4 is more stable *(22,23)*. The helical structure of exendin-4 is stabilized by the compact conformation formed by amino acids 27–39 that form a hydrophobic "Trp-cage fold" feature that caps and stabilizes the helix *(23)*.

Received January 5, 2005; Revised April 7, 2005; Accepted April 13, 2005.
Author to whom all correspondence and reprint requests should be addressed: Máire Doyle, PhD, University of Florida, Department of Oral Biology/Dental Science Building, Box 100424, Rm D5-15, 1600 SW Archer Road, Gainesville, FL 32610-0424. E-mail: medoyle@dental.ufl.edu

**Table 1**
Amino Acids Sequences of the Three GLP-1 Receptor Agonists Studied and the Abbreviations of These Peptides Used in the Text[a]

| | | | | | | | | |
|---|---|---|---|---|---|---|---|---|
| GLP-1 Numbering | | 7 | 11 | 16 | 21 | 26 | 31 | |
| GLP-1 | GLP-1 | HAEGTFTSDVSSYLEGQAAKEFIAWLVKGR | | | | | | |
| Exendin-4 Numbering | | 1 | 5 | 10 | 15 | 20 | 25 | 30 35 |
| Exendin-4 | Ex-4 | HGEGTFTSDLSKQMEEEAVRLFIEWLKNGGPSSGAPPPS | | | | | | |
| Exendin (1–30) | Ex (1–30) | HGEGTFTSDLSKQMEEEAVRLFIEWLKNGG | | | | | | |

[a]The underlined amino acids are the nine amino acids of the C-terminus that are absent from GLP-1 and exendin (1–30).

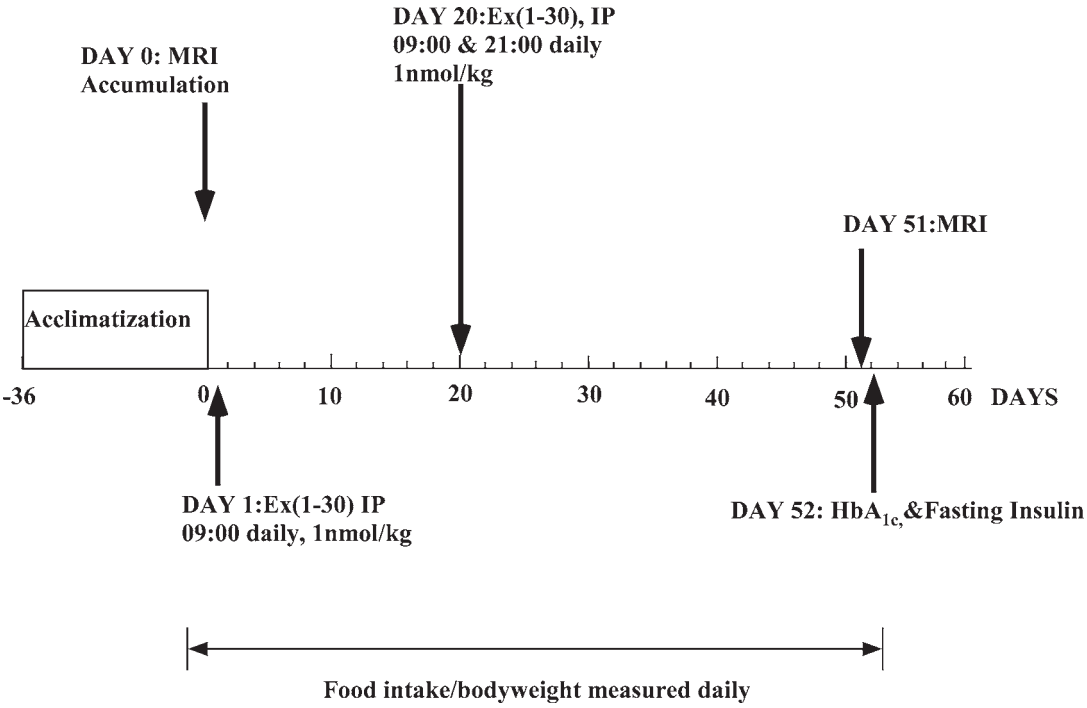


**Fig. 1.** Timeline for chronic Ex (1–30) study in *db/db* mice.

As the nine-amino-acid C-terminal addition to exendin-4 is likely to make it immunogenic in humans, we investigated how the compound exendin (1–30), that is, exendin-4 without the unique C-terminus, functions. Removal of the nine amino acids would also lead to a breakdown in the compact "Trp cage fold." Because of the immunogenic potential of the nine C-terminal amino acids, we wished to examine their biological importance in a model of diabetes and at the same time ascertain their importance for binding of exendin-4 to the GLP-1 receptor. Previously we had compared the truncated exendin (1–30) compound in vitro in terms of its affinity for the GLP-1 receptor and ability to stimulate intracellular cAMP production in vitro, with GLP-1 and exendin-4 *(18)*. We demonstrated that exendin (1–30) had a reduced affinity for the GLP-1 receptor and decreased capacity to stimulate intracellular cAMP production in insulinoma cells. Here we assessed the effects of the truncated exendin-4 compound on weight gain over a period of 51 d by measuring food intake and body weight on a daily basis, as we had done previously with exendin-4 in the same diabetic mouse model *(13)*. We also examined the effect of exendin (1–30) on fat deposition by applying magnetic resonance imaging, a technique we had previously used for exendin-4 treatment in rats *(24)*, to this diabetic mouse model and compared the volume of the subcutaneous and visceral fat compartments at the beginning and at the end of the treatment protocol.

## Results

### *Chronic Study with Ex (1–30) in* db/db *Mice*

Ex (1–30) (1 nmol/kg) was administered once daily at 09:00 h for 20 d to *db/db* mice (Fig. 1). On d 20, blood was drawn from the tip of the tail (between 10:00 and 11:00 h) to ascertain whether Ex (1–30) at the dose and frequency used was lowering blood glucose. Fasting blood glucose values were 410 ± 5 mg/dL for the Ex (1–30)–treated mice and were above the detection limit (600 mg/dL) for those animals receiving saline injections. $HbA_{1C}$ values were also measured and were 7.8 ± 0.4 and 7.7 ± 0.3% for the Ex (1–30)

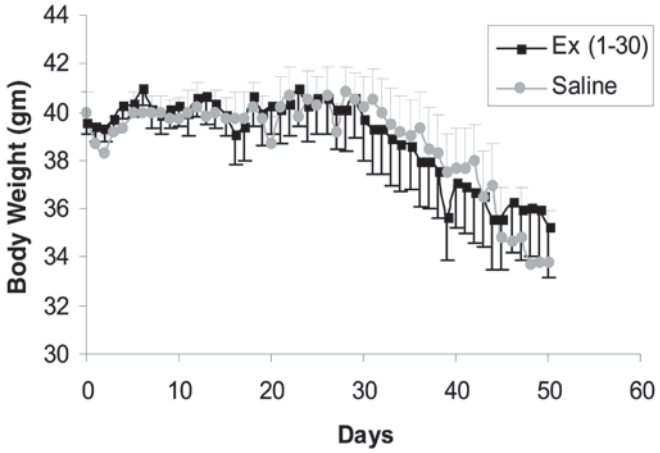


**Fig. 2.** Daily body weights of saline ($n = 6$) and Ex (1–30) treated diabetic mice ($n = 7$). Animals were weighed at the time of their morning injection at 09:00 h. The results are means ± SEM.

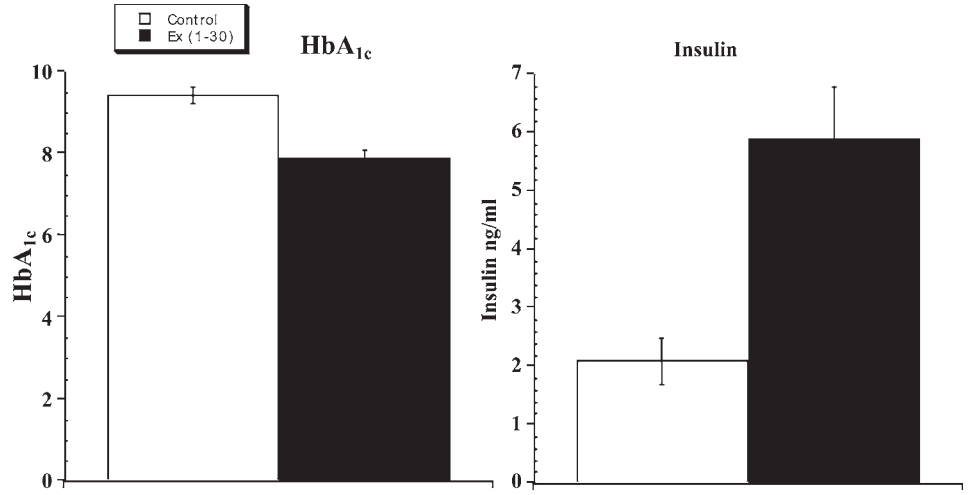


**Fig. 3.** Hemoglobin $A_{1C}$ ($HbA_{1C}$) and insulin concentrations after a 16 h fast in the diabetic mice given Ex (1–30) (1 nmol/kg) or saline intraperitoneally for 51 d.

and saline-treated mice, respectively. As the $HbA_{1C}$ were the same for the treated and control groups, we decided to administer the compound twice a day at 09:00 h and 21:00 h from d 21 onward. The animals were weighed daily, and their food intake was monitored each day at 09:00 h. No significant difference was observed between the food intake of those mice receiving treatment and those receiving saline injections at any point in the study (data not shown). Figure 2 clearly shows that both sets of animals began losing weight by wk 4 of treatment. However, it is noticeable that the animals receiving the Ex (1–30) compound were not losing weight as rapidly as those on saline injections. The $HbA_{1C}$ determined at the end of the study was 7.9 ± 0.2 vs 9.5 ± 0.2% ($p = 0.001$) treated versus con-trol, respectively. Therefore although the treated *db/db* mice were still diabetic, their blood glucose levels were being controlled to a certain extent by the Ex (1–30) treatment. Consequently, the Ex (1–30) group had higher fasting insulin levels at the end of the treatment (Fig. 3) and they did not loose weight to the same degree that the untreated animals did.

To monitor the effects of Ex (1–30) treatment on abdominal fat deposition during treatment, we used MRI to quantify differences in abdominal fat volume that occurred between d 0 and 51, and analyzed differences between the control and treated groups. We measured the fat in both the visceral and subcutaneous compartments of the abdomen. Images of the abdomen and their corresponding histograms gave clear contrast between fat (bright) and non-fat (dark) regions (Fig. 4). Example images are shown of mice from the Ex (1–30) (Fig. 4A,B) and control groups (Fig. 4 C,D) for approximately the same abdominal slice. Corresponding graphs of calculated percentage fat are shown below for each image pair.

The change in the amount of total abdominal fat can be seen when the abdominal fat is expressed as a percentage of the total body fat (Fig. 5A). The means for the control and treated at d 0 were, respectively, 39 ± 1% and 39 ± 4% and d 51, 35 ± 2% and 25 ± 2%, which corresponds to a loss of approx 0.3 g and 1.2 g of abdominal fat in the control and treated groups, respectively. The mean results for each group

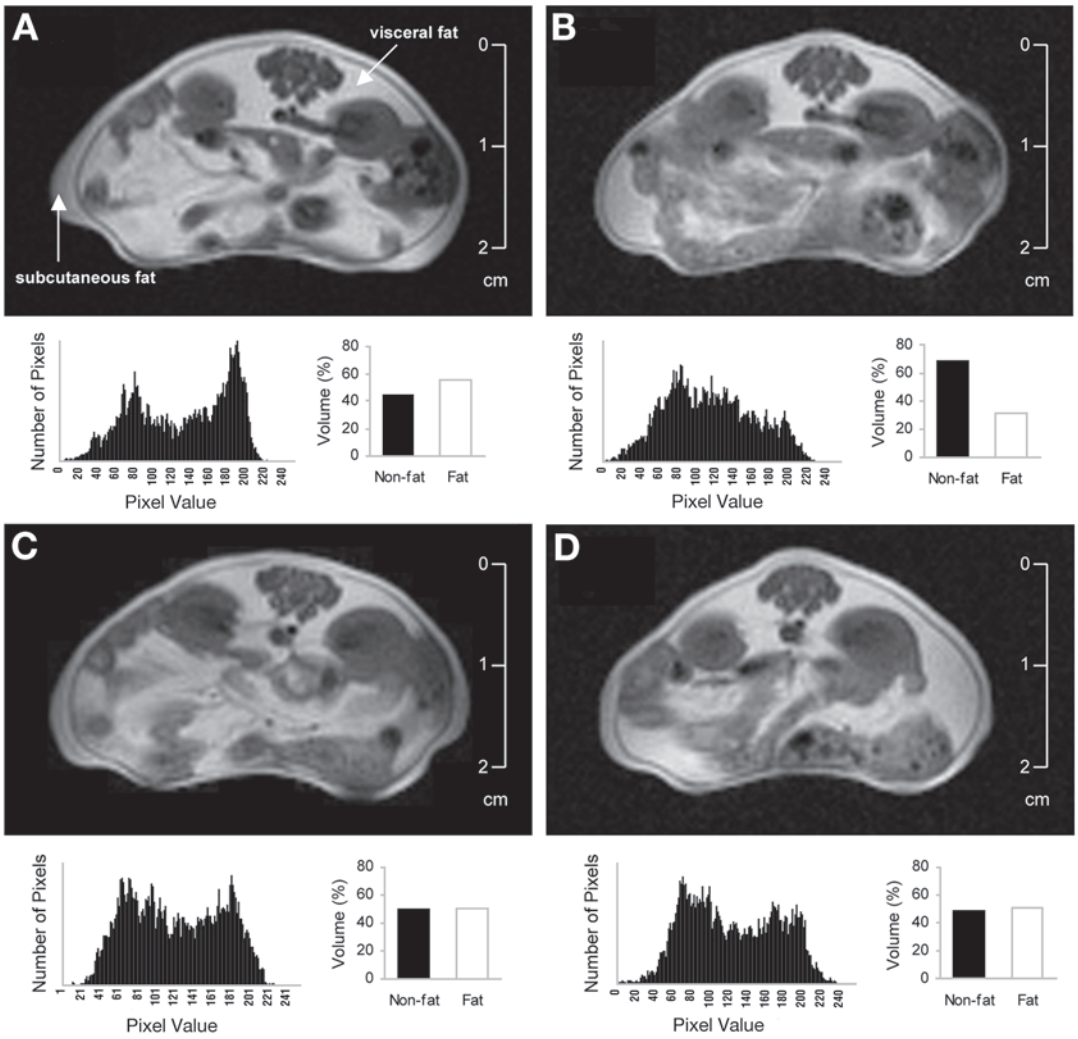


**Fig. 4.** Examples of T1-weighted spin echo images images of the same transverse abdominal slice, for diabetic mice in the Ex (1–30) group at 0 d (**A**) and 51 d (**B**) and in the control group at 0 d (**C**) and 51 d (**D**). The fat tissue is represented by the bright regions, with the darker regions representing non-fat tissue. The visceral and subcutaneous regions are shown, as indicated. Below each image, the corresponding intensity histogram shows the separation between non-fat tissue (low value pixels) and fat tissue (high value pixels). The calculated proportions of non-fat and fat tissue are shown by the corresponding bar graph (non-fat=black bars; fat=white bars). In this slice, a significant decrease in the proportion of total fat is shown in the Ex (1–30) animal. This can be seen to be largely due to fat loss in the visceral fraction, although the amount of subcutaneous fat has also decreased. In the example slices shown for the control animal, there was no decrease in the proportion of total fat volume.

are shown in Fig. 5B, which depicts total, visceral, and subcutaneous abdominal fat lost in each group, as a percentage of the initial total abdominal fat volume. Statistical comparisons showed that over the 51 d period, significant abdominal fat reduction occurred in the visceral fat fraction ($p$ = 0.003), leading to a significant reduction in total abdominal fat volume ($p$ = 0.0012). In the control group, however, there was no significant reduction in total fat or visceral fat volumes as measured over the abdomen. It was noted that the control animals lost more fat in the chest region than did the treated animals, accounting for the greater loss in body weight in the control animals (Fig. 2). In both groups, non-significant reductions in subcutaneous abdominal fat were measured [Ex (1–30): $p$ = 0.06; Control: $p$ = 0.051]. Between-group comparisons showed significantly greater total fat reduction ($p$ = 0.04) and visceral fat reduction ($p$ = 0.005) in the treated animals.

### *The Effects of Ex (1–30) on β-Cell Area and Proliferation in the Fisher Rat Pancreas*

We then assessed the effects of a once daily injection of Ex (1–30) (1 nmol/kg) on β-cell proliferation and total β-cell area in the pancreas of 3-mo-old Fisher rats treated for 4 and 8 d. A comparison was made with saline-treated controls in each case. We did not observe a difference between controls of either treatment group, so the results from these two control groups were pooled. There was no difference in total β-cell area between any of the groups (results not

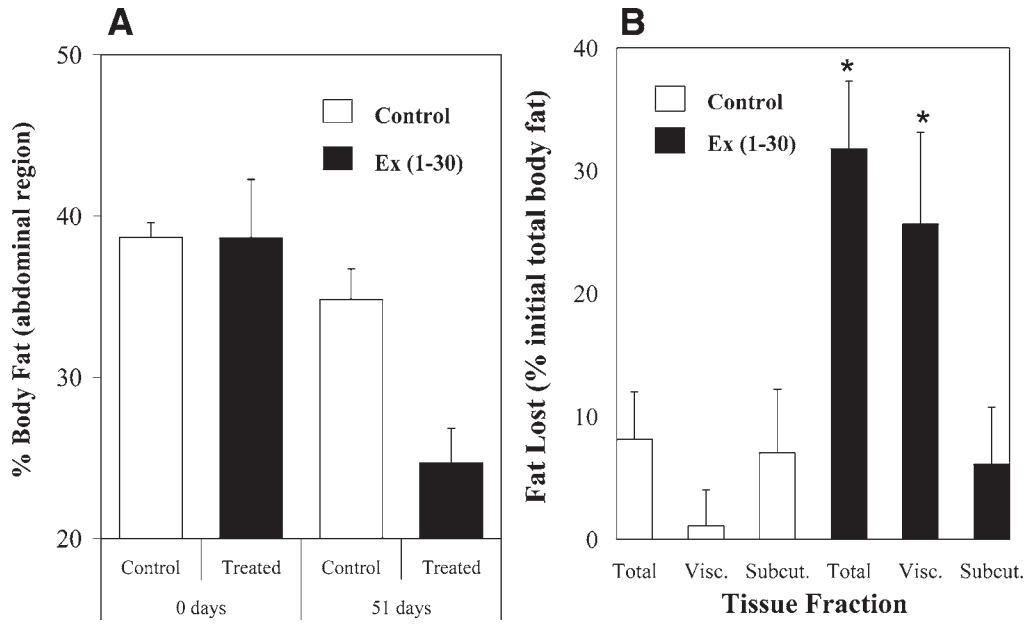


**Fig. 5.** (**A**) Abdominal fat volume shown as a percentage of total fat for Ex (1–30)–treated ($n = 6$) and control animals at d 0 and d 51 ($n = 6$) of treatment. (**B**) Abdominal fat volume that the diabetic mice lost over 51 d, expressed as percentage of the initial total fat volume (0 d), shown for the Ex (1–30) treatment group ($n = 6$, black bars) and the control group ($n = 5$, white bars). For each group, total fat lost, as well as the fat lost from the visceral (visc.) and subcutaneous (subcut.) tissue fractions, is shown. *$p < 0.05$ Ex (1–30) vs control. The data show that there was a significantly greater volume of total fat and visceral fat lost in the Ex (1–30)–treated animals than in the control animals. Both groups showed decreased total fat volume at the 51 d time point. In the control group, this loss was largely due to loss of fat from the subcutaneous fraction, which occurred to a similar extent in the treated animals.

shown). There was no significant difference in the number of BrdU-positive nuclei per islet when a comparison was made between the pancreata of the animals receiving 4 d of treatment and those receiving saline injections. There was, however, a significant difference ($p = 0.03$) between the 8 d treatment and the controls for which the values were respectively 10.7 ± 1.8% and 6.5 ± 0.5%, respectively, in terms of the percentage of islets with BrdU-positive nuclei. A representative example of one of these islets is shown in Fig. 6.

## Discussion

Here we demonstrate the importance of the nine C-terminal amino acids of exendin-4 to its increased affinity to the GLP-1 receptor (relative to GLP-1) and its potency in vivo. Truncation of the N-terminus of exendin-4 up to residue number 9 does not result in loss of receptor affinity *(12)*. However, with respect to both exendin-4 and GLP-1 the first two amino acids are important for biological activity with N terminally truncated exendin-4 compounds being potent antagonists of the GLP-1 receptor *(12,17)*. Exendin-4 and GLP-1 have eight amino acids in common in the central region of the molecule (between residues 10–30 in exendin-4 and 16–26 in GLP-1). These common residues are also on the same face of the α-helix *(22,23)*. Residues 7, 10, 12, 13, 15, 28, and 29 of GLP-1 are known to be essential for receptor binding, and these residues are also common to both agonists *(26)*. The parity between the structure and function relationships of the central helical regions of the two peptides and the increased affinity of the N terminally truncated exendin derivatives for the GLP-1 receptor implies that exendin-4 must have an additional feature in the C-terminus that contributes to its increased affinity for the GLP-1 receptor. The recent NMR study from Neidigh and colleagues points to the increased helical stability in the solution structure of exendin-4 relative to GLP-1 which is stabilized by the "Trp cage" feature in the C-terminus of exendin-4 *(23)*, as the factor. However, previous to our report *(18)* no studies were performed to analyze the importance of this part of the molecule to the activity and binding of exendin-4. Here we show that disruption of the "Trp cage" by removal of the last nine amino acids of exendin-4 results in compound that is not as potent in vivo as the parent compound. Previously we had shown that the binding of exendin (1–30) was comparable to that of GLP-1 itself *(18)*. In fact no C-terminal truncated version of exendin-4 or any GLP-1 peptide we have tested is as effective as exendin-4 in binding to the GLP-1 receptor *(18)*.

Long-term treatment of *db/db* mice with exendin (1–30) had beneficial effects on glucose tolerance in that there was a reduction in $HbA_{1C}$ and fasting blood glucose levels, which was coupled with an increase in fasting insulin levels. The $HbA_{1C}$ of the animals treated for 51 d with exendin (1–30) was significantly lower than that in animals receiving saline injections (control 9.5 ± 0.2% and treated 7.9 ± 0.2%). $HbA_{1C}$ is a measure of the severity of diabetes reflecting

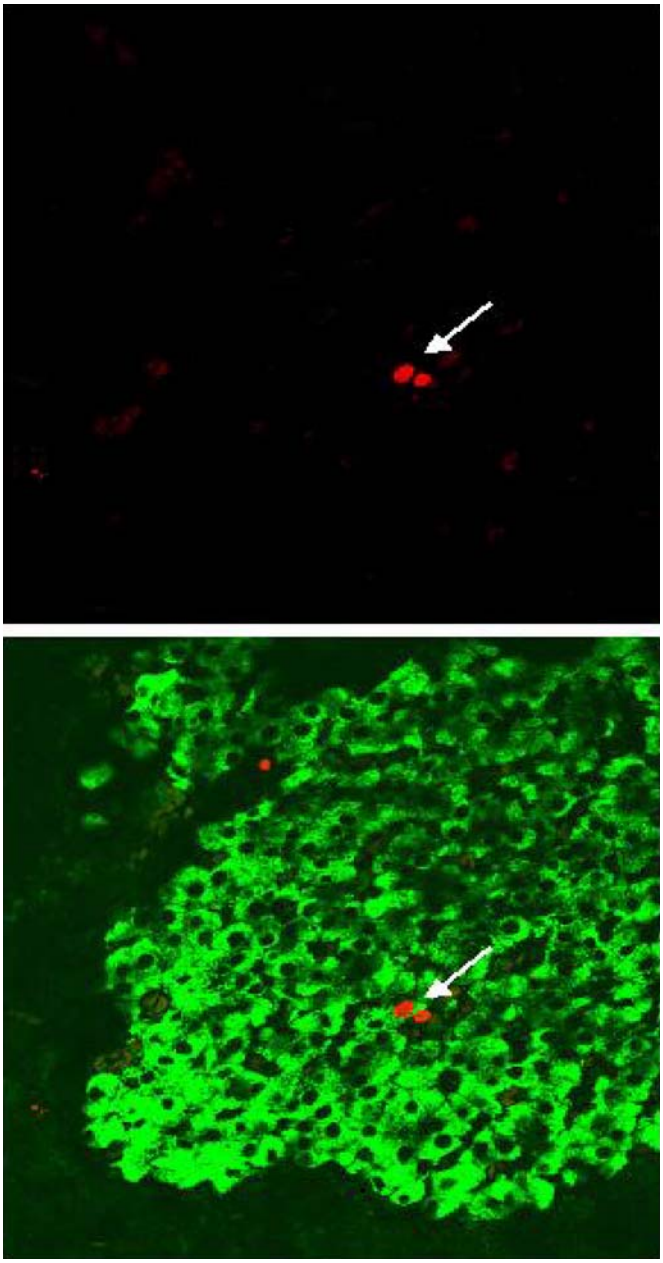

**Fig. 6.** Proliferation of β-cells in Ex (1–30) treated rats. Laser scanning confocal microscopy images of two BrdU (+) β-cells (arrows) from a 2-mo-old Fisher rat [treated for 8 d with Ex (1–30), 1 nmol/kg, sc] pancreatic islet, double-stained for BrdU and insulin, with (top panel) and without (bottom panel) color separation by means of the Metamorph software (40× magnification).

the mean elevation in blood glucose. Based on this criterion, exendin (1–30) is not as effective as exendin-4 in consistently maintaining low blood glucose values. A reduction of the $HbA_{1C}$ levels to normal levels was observed in *db/db* mice on twice daily injections at similar concentrations of exendin-4 *(13)*. Although these *db/db* mice were treated at a different time with exendin-4, they demonstrated a 53% reduction (8.8% control, 4.7% exendin-4 treated, ref. *13*) in their $HbA_{1C}$ compared with the 17% reduction seen here with exendin (1–30). The reduced effectiveness of exendin (1–30) can be correlated to its lower affinity for the GLP-1 receptor and the lower amounts of cAMP that it generates in insulin secreting cells.

Our MRI analysis of the fat deposition in the abdomen shows that there was a significant reduction in total abdominal fat in the exendin (1–30)–treated mice compared to the controls. This was predominantly due to a reduction in the volume of the visceral fat compartment. This would suggest that exendin (1–30) treatment preferentially targeted the abdominal visceral fat tissue. Although there was a small reduction in the total abdominal fat in the control animals as well, this was largely due to loss of fat from the subcutaneous fraction, which occurred to a similar extent in both groups. We also examined MRI data taken from regions of the animals other than the abdomen (data not shown). Both control and treated groups demonstrated a reduction in the amount of fat in the chest and tail regions. This would also have contributed to the similar weight loss measured in each group. Thus, although both groups of animals lost weight, only those receiving exendin (1–30) actually demonstrated a significant reduction in the volume of the abdominal fat compartment. Chronic treatment with Ex (1–39) reduces fat deposition in both the visceral and subcutaneous fat compartments of the abdomen of Zucker rats, which also express a defective leptin receptor *(24)*.

Previously we had shown that GLP-1 receptor agonists are capable of increasing β-cell proliferation and area in rodents *(7,8)*. Here we investigated if the truncated compound would have similar effects. Treatment of 2-mo-old Fisher rats, for either 4 or 8 d with exendin (1–30) did not result in an increase in β-cell area. However, exendin (1–30) increased β-cell proliferation at the 8-d treatment point. Previously, with a continuous infusion of GLP-1 to old Wistar rats we observed an increase in β-cell mass after 5 d of treatment but not after 3 d, with increased proliferation evident at 2 d *(7)*. It is possible that we did not observe an increase in β-cell mass with exendin (1–30) as the increase in β-cell proliferation that we observed had not yet begun to effect the β-cell mass. It is known from earlier studies with exendin-4 that a significant expansion of β-cell mass is not observed until 14 d or longer following initiation of exendin-4 treatment *(8,27)*. It is also possible that the lack of effect on β-cell mass and the small effect on β-cell proliferation seen in these animals is due to the use of animals with normal glucose tolerance that already have an adequate β-cell mass.

In summary, we have shown that while the PSSGAPPPS sequence of exendin-4 is not essential for biological activity, its removal markedly reduced the affinity for the GLP-1 receptor *(18)* and the biological effectiveness of the compound when administered long term. Further pharmacokinetic studies on exendin (1–30) are required to determine the extent to which the resistance to DPP IV degradation contributes to the increased stability and potency of exendin-4. Our study

would seem to imply that the increased affinity of exendin-4 for the GLP-1 receptor is a significant factor in its increased potency.

## Materials and Methods

The peptide exendin (1–30) [Ex (1–30)] was synthesized by Gemini Biotech (The Woodlands, TX), and its purity was confirmed by high-performance liquid chromatography. Table 1 shows the sequences of this peptide. Plasma insulin levels were assayed by ELISA (Crystal Chem Inc., Chicago IL). We assayed $HbA_{1C}$ with a Bio-Rad (Hercules, CA, USA) DiaSTAT machine, which uses low-pressure cation exchange chromatography in conjunction with gradient elution to separate hemoglobin subtypes and variants from hemolyzed blood. The separated hemoglobin fractions were monitored by means of absorption of light at 415 nm. Blood glucose levels were measured using a Glucometer Elite (Bayer Diagnostics, Tarrytown, NY).

### *Animals*

Two-month-old Fisher rats (Harlan, Indianapolis, IN) were used in the acute experiments and 2-mo-old *C57BLKS/J-Lepr$^{db}$/Lepr$^{db}$* mice (Jackson Laboratories, Bar Harbor, ME) were used in the chronic experiments. All animals were cared for in accordance with protocols approved by the Animal Care and Use Committee of the Gerontology Research Center, National Institute on Aging (Baltimore, MD). They were allowed *ad libitum* access to chow and water. Animals were on a 12 h light–dark cycle (lights on 07:00). The bedding for the *db/db* mice was a paper-based product, Carefresh (Absorption Co., Belingham, WA) and the Fisher rats were housed on Beta Chip bedding (Northeastern Products Corporation, Warrensburg, NY).

### *Chronic Study with Ex (1–30) in* db/db *Mice*

Protocol (Fig. 1). Animals were housed in our facilities for 2.5 mo to facilitate their acclimatization before the start of the experiment. For the first 20 d of treatment the animals were given Ex (1–30) (1 nmol/kg; $n = 7$) ip injection daily at 09:00 and a separate group of mice received saline alone ($n = 6$). Thereafter, animals received ip Ex (1–30) (1 nmol/kg) or saline at approx 09:00 and 21:00 for the following 31 d. At the end of the first 20 d of the treatment protocol, fasting blood glucose levels and $HbA_{1C}$ were measured. Food intake and animal weight were determined daily at the time of the 09:00 injection. No day was missed in the schedule. Magnetic resonance images (MRI) were acquired on d 0 and 51. On d 52, blood was taken for $HbA_{1C}$ and insulin levels. One mouse from each treatment group died either upon anesthesia prior to or during the MRI procedure on d 51.

### *Magnetic Resonance Imaging*

Magnetic resonance images were obtained using a 1.9 T, 31 cm bore Bruker BioSpec system (Bruker Medizintechnik GmbH, Ettlingen, Germany), with a 20 cm inner diameter shielded gradient set and a 5 cm diameter volume resonator. The animals were anesthetized with isofluorane and standard T1 weighted multislice spin-echo images (TR = 500 ms, TE = 8.5 ms) were obtained over 20 contiguous transverse slices of thickness 2.1 mm each, covering a region from the chest to the beginning of the tail. The field of view was $5 \times 5$ cm over $128 \times 128$ pixels. Each image was acquired using eight averages, over a total imaging time of approx 9 min. Imaging was performed on all animals at two time points (d 0 and d 51).

Separation of visceral and subcutaneous regions was performed (Bruker Paravision software) by drawing regions of interest (ROIs) for each slice. Segmentation of adipose from normal tissue was achieved using intensity histograms derived from each ROI (NIH Image software, National Institutes of Health, USA). The histograms generally showed two well-separated peaks (corresponding to water and adipose tissue), which were isolated using the valley between them as the demarcation point *(27)*, enabling the adipose tissue content in each ROI to be summed.

### *Treatment Protocol and Tissue Preparation*

Two-month-old Fisher rats acclimatized to our facilities for 1 mo were used in this experiment. One group received an ip injection of Ex (1–30) (1 nmol/kg; $n = 3$) or saline ($n = 2$) for 4 d and another group received Ex (1–30) (1 nmol/kg; $n = 7$) or saline ($n = 2$) for 8 d. Six hours prior to being sacrificed, the rats were injected with 5-bromo-2'deoxyuridine (BrdU; Sigma, St. Louis, MO), 100 mg/kg ip. Each rat was sacrificed, its pancreas was excised, cleared of fat and lymph nodes, blotted, weighed, and fixed in 4% paraformaldehyde in 0.1 *M* phosphate buffer (pH 7.4) overnight and stored in 70% ethanol until processing. The pancreatic tissue was routinely processed and embedded in paraffin. Sections of pancreas were cut at 5 microns and placed on poly-L-lysine coated slides (Fisher, Springfield, NJ), air dried overnight, and then placed in a 60°C oven for 30 min.

### *Immunoperoxidase Staining for Insulin*

All primary and secondary antibodies were diluted in 10% normal goat serum (Vector Laboratories, Burlingame, CA) with 0.3% Tween in PBS. The slides were deparaffinized, hydrated to distilled water, and placed in three changes of PBS for a total of 10 min. Endogenous peroxidase was blocked using 5% hydrogen peroxide in absolute methanol for 10 min at room temperature followed by a 5 min wash in distilled water, then a 5 min wash in PBS. They were blocked with 3% BSA and 0.1% Tween solution (Sigma, St. Louis, MO) for 1 h at room temperature, followed by three washes in PBS for 2 min each. The primary antibody, guinea pig anti-human insulin (Linco, St. Charles, MO cat. no. 4011-01F, lot no. H46P-F) was used at a 1:300 dilution for 1 h at room temperature. The sections were then washed in three changes of PBS for a total of 10 min, followed by an incu-

bation with a HRP conjugated rabbit anti-guinea pig secondary antibody (Zymed Laboratories South San Francisco, CA, cat. no. 61-4620, lot no. 20370082) used at a 1:40 dilution for 10 min at room temperature. The reaction was developed using DAB (3'3-diaminobenzidine) chromogen (Vector Laboratories, Burlingame, CA) for 2 min at room temperature, followed by a deionized water wash and a Harris hematoxylin counterstain (Poly Scientific, Bay Shore, NY) for 2 min. The slides were then dehydrated, cleared and mounted with Permount (Fisher). To confirm specific staining, the tissue was incubated with insulin antibody that was pre-absorbed overnight with insulin (100 μ*M*); control slides were incubated with vehicle alone and no primary antibody.

### *Immunofluorescence Staining for BrdU and Insulin*

Following rehydration, sections were treated with 0.125% trypsin (Zymed, So. San Francisco, CA) in a moist chamber for 10 min. They were washed three times with distilled water and then treated with a denaturing solution (Zymed) for 25 min at room temperature. They were then washed and blocked as above. Sections were incubated with an anti-rat BrdU IgG2a [Clone BU1/75 (ICR1) 2.5 μg/mL, Accurate Chemical and Scientific Corporation, Westbury, NY] for 1–2 h at room temperature, and washed and incubated with an Alexa Fluor 568 goat anti-rat IgG (Molecular Probes, Eugene, OR) (2 μg/mL) for 1 h at room temperature, and washed and incubated with the anti-insulin IgG as above. Following washing they were incubated at room temperature for 1 h with Alexa Fluor 488 goat anti-guinea pig IgG (Molecular Probes) (2 μg/mL). Slides were mounted with Vectashield medium (Vector Laboratories). Control slides were incubated with vehicle alone and no primary antibody.

### *Laser Confocal Scanning Microscopy*

Cells were imaged with a Zeiss LSM-410 inverted confocal microscope (Carl Zeiss, Inc., Thornwood, NJ). Images of five random section fields were analyzed in each slide. The AlexaFluor fluorescent antibodies were excited with either the 488-nm line of a krypton–argon laser and recorded at the presence of emission filter BP 515–565 nm or with the 568-nm laser line and recorded at the presence of an emission filter BP 590–610 nm. The microscope objective was a Zeiss 63× NA 1.4 oil immersion, and the confocal pinhole was set to obtain spatial resolution of 0.4 μm in the horizontal plane and 1 μm in the axial dimension. Image processing, integrated morphometry analysis, and final presentation were done using the MetaMorph 4.6.3. software (Universal Imaging, Inc., West Chester, PA).

### *Determination of β-Cell Area*

Sectioned tissue images were acquired through a 2.5× objective of a phase-contrast light microscope (Carl Zeiss Inc., Thornwood, NJ) and digitized by means of a Sony Power HAD digital camera. The total pancreatic area for every section image was quantified (an average of 20 per section) using MetaMorph 4.6.3. software (Universal Imaging, Inc.). Total β-cell area was determined by utilizing software region measurements after having manually highlighted each individual area that was positive for insulin in the image under study. In all cases, the system was calibrated for both total pancreatic and regional measurements using a stage mount. No difference was evident in the pancreata of the saline-treated groups from the two different time points, so their data were pooled.

### *Determination of β-Cell Replication*

The percentage of islets with cells double-labeled with BrdU and insulin were counted with a Nikon Diaphot inverted phase-contrast microscope equipped with a fluorescence attachment system (Nikon, USA) using a 20 × 0.4 objective. Four sections were examined in the case of each rat, with the number of insulin-positive clusters per section being 102.7 ± 7.6. The mean was calculated for each rat and then averaged over treated and control separately. No difference was evident in the pancreata of the saline-treated groups from the two different time points, so their data were pooled.

### *Statistical Analysis*

All values are shown as the mean ± SEM, and the differences among the groups in the MRI analysis were analyzed using ANOVA and for the analysis on the percentage of BrdU-positive cells, an unpaired *t*-test with Welch correction for unequal variances was performed.

## Acknowledgments

Without the positive on-going support of our scientific director, Dr. D. L. Longo, these studies would not have been conducted. Michael J. Theodorakis was supported by a Clin PRAT Fellowship from the National Institute of General Medical Sciences and the NIH Clinical Center, Bethesda, MD. The current address of Patrick McConville is Molecular Imaging Research, Inc. (MIR), 924 North Main Street, Ann Arbor, MI 48104.

## References

1. Doyle, M. E. and Egan, J. M. (2001). *Recent Prog. Horm. Res.* **56,** 377–399.
2. Kieffer, T. J. and Habener, J. F. (1999). *Endocr. Rev.* **20,** 876–913.
3. Willms, B., Werner, J., Holst, J. J., Orskov, C., Creutzfeldt, W., and Nauck, M. A. (1996). *J. Clin. Endocrinol. Metab.* **81,** 327–332.
4. Komatsu, R., Matsuyama, T., Namba, M., et al. (1989). *Diabetes* **38,** 902–905.
5. Prigeon, R. L., Quddusi, S., Paty, B., and D'Alessio, D. A. (2003). *Am. J. Physiol. Endocrinol. Metab.* **285,** E701–E707.
6. Wang, Y., Egan, J. M., Raygada, M., Nadiv, O., Roth, J., and Montrose-Rafizadeh, C. (1995). *Endocrinology* **136,** 4910–4917.
7. Perfetti, R., Zhou, J., Doyle, M. E., and Egan, J. M. (2000). *Endocrinology* **141,** 4600–4605.

8. Stoffers, D. A., Kieffer, T. J., Hussain, M. A., et al. (2000). *Diabetes* **49,** 741–748.
9. Zander, M., Madsbad, S., Madsen, J. L., and Holst, J. J. (2002). *Lancet* **359,** 824–830.
10. Drucker, D. J. (2001). *Curr. Pharm. Des.* **7,** 1399–1412.
11. Orskov, C., Rabenhoj, L., Wettergren, A., Kofod, H., and Holst, J. J. (1994). *Diabetes* **43,** 535–539.
12. Montrose-Rafizadeh, C., Yang, H., Rodgers, B. D., Beday, A., Pritchette, L. A., and Eng, J. (1997). *J. Biol. Chem.* **272,** 21201–21206.
13. Greig, N. H., Holloway, H. W., De Ore, K. A., et al. (1999). *Diabetologia* **42,** 45–50.
14. Parkes, D., Jodka, C., Smith, P., et al. (2001). *Drug Dev. Res.* **53,** 260–267.
15. Egan, J. M., Clocquet, A. R., and Elahi, D. (2002). *J. Clin. Endocrinol. Metab.* **87,** 1282–1290.
16. Thum, A., Hupe-Sodmann, K., Goke, R., Voigt, K., Goke, B., and McGregor, G. P. (2002). *Exp. Clin. Endocrinol. Diabetes* **110,** 113–118.
17. Thorens, B., Porret, A., Bühler, L., Deng, S. P., Morel, P., and Widmann, C. (1993). *Diabetes* **42,** 1678–1682.
18. Doyle, M. E., Theodorakis, M. J., Holloway, H. W., Bernier, M., Greig, N. H., and Egan, J. M. (2003). *Reg. Pep.* **114,** 153–158.
19. Egan, J. M., Meneilly, G. S., and Elahi, D. (2003). *Am. J. Physiol. Endocrinol. Metab.* **284,** E1072–E1079.
20. Nielsen, L. L. and Baron, A. D. (2003). *Curr. Opin. Investig. Drugs* **4,** 401–405.
21. Kolterman, O. G., Buse, J. B., Fineman, M. S., et al. (2003). *J. Clin. Endocrinol. Metab.* **88,** 3082–3089.
22. Andersen, N. H., Brodsky, Y., Neidigh, J. W., and Prickett, K. S. (2002). *Bioorg. Med. Chem.* **10,** 79–85.
23. Neidigh, J. W., Fesinmeyer, R. M., Prickett, K. S., and Andersen N. H. (2001). *Biochemistry* **40,** 13188–13200.
24. Szayna, M., Doyle, M. E., Betkey, J. A., et al. (2000). *Endocrinology* **141,** 1936–1941.
25. Adelhorst, K., Hedegaard, B. B., Knudsen, L. B., and Kirk, O. (1994). *J. Biol. Chem.* **269,** 6275–6278.
26. Xu, G., Stoffers, D. A., Habener, J. F., and Bonner-Weir, S. (1999). *Diabetes* **48,** 2270–2276.
27. Ishikawa, M. and Koga, K. (1998). *Magn. Reson. Imaging* **16,** 45–53.